

ORIGINAL ARTICLE

Correlation analysis of expressions of PTEN and p53 with the value obtained by magnetic resonance spectroscopy and apparent diffusion coefficient in the tumor and the tumor-adjacent area in magnetic resonance imaging for glioblastoma

Yunyun Li^{1*}, Feng Ji^{1*}, Yuzhi Jiang¹, Ting Zhao¹, Chongfu Xu²

¹Department of Radiology and ²Department of Neurosurgery, Liaocheng People's Hospital, Liaocheng, Shandong 252000, China

*These authors contributed equally to this study

Summary

Purpose: To explore the correlation of the expression levels of phosphate and tension homology deleted on chromosome ten (PTEN) and p53 of glioblastoma multiforme (GBM) with the value obtained by magnetic resonance spectroscopy (MRS) and apparent diffusion coefficient (ADC) in the tumor and the tumor-adjacent area in magnetic resonance imaging (MRI).

Methods: A total of 38 patients were operated for GBM. All the patients had received diffusion-weighted imaging (DWI) and MRS prior to surgery. ADC of water molecules and values of metabolite indexes of MRS, including n-acetyl aspartate (NAA), choline (Cho) and creatine (Cr), were recorded, and the ratios of Cho/NAA, Cho/Cr and NAA/Cr were calculated. Hematoxylin-eosin (H&E) staining was done to examine the morphology of tumor and of tumor-adjacent tissues; immunohistochemistry (IHC) was performed to examine the expressions of PTEN and p53 in the tumor and the tumor-adjacent area. Finally, the correlations of the expressions of PTEN and p53 with ADC, Cho/NAA, Cho/Cr and NAA/Cr of the tumor and the tumor-adjacent area were analyzed.

Results: H&E staining showed that GBM tissues had disordered morphology, different sizes of cells, large cell nuclei and significant cell heterogeneity. IHC indicated that the expression level of p53 protein in the tumor was significantly

higher than in the tumor-adjacent tissues ($p < 0.05$). The expression level of PTEN protein was high in the tumor-adjacent tissues, but significantly deficient in the tumor. DWI showed that the signal of DWI in the tumor was significantly increased, but ADC was decreased compared with the tumor-adjacent area. MRS indicated that the wave band of Cho in the tumor was significantly increased, NAA was significantly lowered, and Cr section was decreased compared with the tumor-adjacent area, while NAA/Cr in the tumor was significantly decreased compared with the tumor-adjacent area ($p < 0.05$). Correlation analysis indicated that PTEN levels in the tumor and the tumor-adjacent area were positively correlated with ADC in the corresponding area, while p53 in the tumor and the tumor-adjacent area was negatively correlated with ADC in the corresponding area. Cho/NAA and Cho/Cr in the tumor were positively correlated with p53 in the tumor, but negatively correlated with PTEN in the tumor. However, NAA/Cr of the tumor was irrelevant to the levels of PTEN and p53.

Conclusions: The test results of DWI and MRS of patients with GBM can accurately reflect the inactivation or mutation of PTEN and p53.

Key words: brain glioma, diffusion weighted imaging, magnetic resonance spectroscopy, p53, PTEN

Introduction

Glioblastoma multiforme (GBM) accounts for 40% of all the primary tumors of the central nervous system [1]. The survival time of patients with

GBM (grade IV) is only 15 months [2]. As the therapeutic time window of GBM is short, and there is no space for wrong diagnosis, the characteristics

of GBM must be assessed accurately and rapidly. The anti-oncogenes (PTEN and p53) are the most commonly inactivated or mutant genes in human cancers. Currently, a large number of studies have demonstrated that the progression of patients with GBM is significantly associated with inactivation of PTEN and mutation of p53 [3,4].

At present, the functional MRI that is used widely in clinical imaging diagnosis includes DWI and MRS. In recent years, DWI and MRS have been widely used for the detection of diseases of the central nervous system [5]. DWI can reflect the dispersion of water molecules in the area of the lesion, thus diagnosing the disease [6]. MRS is currently the only way to perform noninvasive testing of metabolites (NAA, Cho and Cr) *in vivo*, and the metabolism of the lesion can be reflected through the change in wave peak [7]. Both of them can provide important information for imaging differential diagnosis of craniocerebral diseases.

This study aimed to analyze the correlations of DWI and MRS in the GBM and the GBM-adjacent area with PTEN and p53, and explore the feasibility of combining molecular diagnostics with imaging to improve the diagnostic efficiency of GBM.

Methods

General data

A total of 38 patients (21 males and 17 females) with GBM that were subjected to operations in the Oncology Department of our hospital from December 2013 to December 2016 were selected. The average age of the patients was 53.5 ± 10.3 years. All the patients with GBM had craniotomy and tumor resection and were pathologically diagnosed with GBM. Twenty-three patients were diagnosed with III-IV, and the remaining 15 with stage I-II according to the World Health Organization (WHO) staging classification. None of them had undergone operation for brain tumor in the past, and they did not receive chemotherapy, radiotherapy or other treatments before enrollment. All the patients had DWI and MRS examinations performed before operation. The general data of the included patients had no statistical differences. This study was approved by the Ethics Committee of our hospital and all of the subjects signed informed consent.

Magnetic resonance examination

DWI examination: 3T MRI system [signal 3T; General Electric (GE) Medical Systems, Milwaukee, Wisconsin, USA] and a circularly polarized head coil were used. The system was equipped with high-performance gradient (40 mT/ms; conversion rate: 150 mT/m/s). The patients laid in supine position and conventional axial [spin echo (SE) sequence] MR plain scan was firstly performed; then, enhanced lateral and sagittal T1-weighted imaging (3,000 s/mm²) were performed. Finally, transverse plain T2-weighted imaging, fast liquid attenua-

tion inversion recovery sequence (FLAIR) imaging and enhanced T1-weighted imaging were carried out.

¹H-MRS examination: Syngo MR 2002B spectrum workstation was adopted to localize the measurement area of ¹H-MRS on the basis of MRI. The surface with maximum area of the tumor was taken as the scanning surface for localizing MRS. Point-resolved spectral sequence was used to measure the tumor area and contralateral area of normal brain tissues: time of repetition (TR): 1,500 ms; time of echo (TE): 135 ms; automatic shimming; layer thickness: 10 mm; layer spacing: 2 mm; field of view (FOV): 240 mm×240 mm; number of excitation (NEX): 1; phase matrix: 160×160; imaging time: 260 s. The metabolic spectrum was obtained simultaneously using the software package (FuncTool) of the spectrometer. The areas under the wave peaks of metabolites including NAA (2.02 ppm), Cho (3.2 ppm) and Cr (3.02 ppm) and the ratios of NAA/Cho, NAA/Cr and Cho/Cr were calculated. The results were expressed as mean ± standard deviation.

Hematoxylin-eosin histopathological examination

GBM tissues and GBM-adjacent tissues were fixed overnight in 4% paraformaldehyde (Google Biology, Wuhan, China) with 10 times volume. Paraffin sectioning (thickness: 0.4 μm) was performed after dehydration and embedding. The sections were baked in an oven at 65°C for 3 hrs. Then dewaxing, gradient ethanol rehydration, staining with H&E, gradient alcohol rehydration and drying were conducted for the sections. Finally, they were sealed with neutral balsam and placed under the microscope (DM-5000B, Leica, Wechsall, Germany) for observation of morphology and photographing.

Immunohistochemical examination

The sections of the tumor tissues and the tumor-adjacent tissues with a thickness of 0.4 μm were placed in citrate buffer solution (100°C) for antigen retrieval for 20 min → incubated in 3% hydrogen peroxide for 10 min to block nonspecific background staining induced by endogenous peroxidase → sealed for 30 min in 5% bull serum albumin (BSA) → incubated at 37°C for 1-2 hrs after the primary-antibody working fluids (PTEN and p53) were added (dilution ratio: 1:200, Santa Cruz, California) → washed with phosphate buffered saline with Tween 20 (PBST) for 3 times → incubated at room temperature for 1 hr after secondary antibody labeled with biotin was added (dilution ratio: 1:500, Santa Cruz, California) → developed with 3, 3'-diaminobenzidine (DAB) substrate kit → redyed with hematoxylin → dehydrated and sealed. The sections were placed under the microscope (Leica) for observation and photographing (at least three areas for each section). Image Pro-Plus 5.0 software (Media Cybernetics, USA) was used to calculate the optical density (OD) of each section.

Statistics

All the results of this experiment were analyzed by MedCalc software (Mariakerke, Belgium). All quantitative data were expressed as mean±SD, and paired t-test was used for the detection of differences among each

index. $P < 0.05$ suggested that the differences were statistically significant.

Results

Observation of morphology of GBM tissues and GBM-adjacent tissues with H&E examination

As shown in Figure 1, GBM tissues had disordered morphology, different sizes of cells, large nuclei and significant cell heterogeneity, while the GBM-adjacent tissues had normal structures.

Analysis of expressions of p53 and PTEN in the tumor tissues and the tumor-adjacent tissues with IHC examination

As shown in Figure 2, p53 was localized in the cell nucleus, while PTEN was localized in the cytoplasm. The expression of p53 protein in tumor tissues was significantly higher than that in tumor-adjacent tissues ($p < 0.05$). The expression of PTEN protein was high in tumor tissues, but significantly deficient in tumor-adjacent tissues ($p < 0.05$) (Table 1).

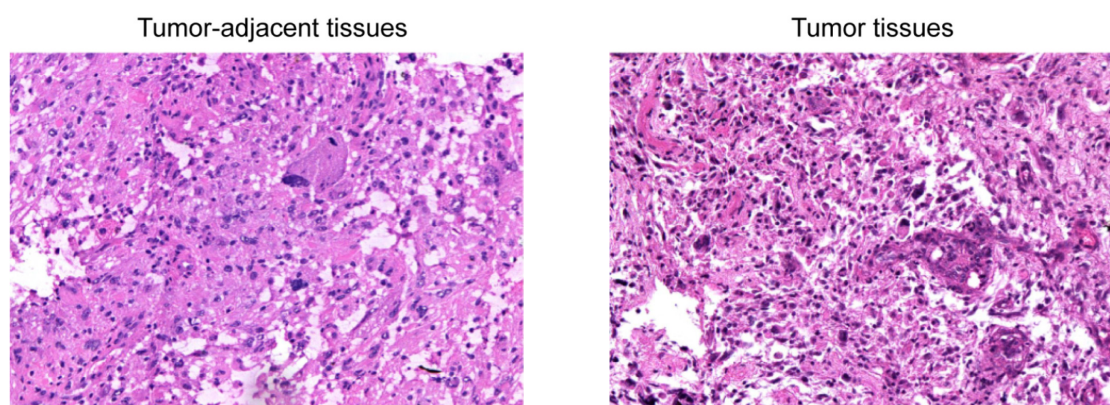


Figure 1. H&E staining of GBM tissues and GBM-adjacent tissues (magnification x40). Compared with GBM-adjacent tissues, GBM tissues had disordered morphology, different sizes of cells, large cell nuclei and significant cell heterogeneity.

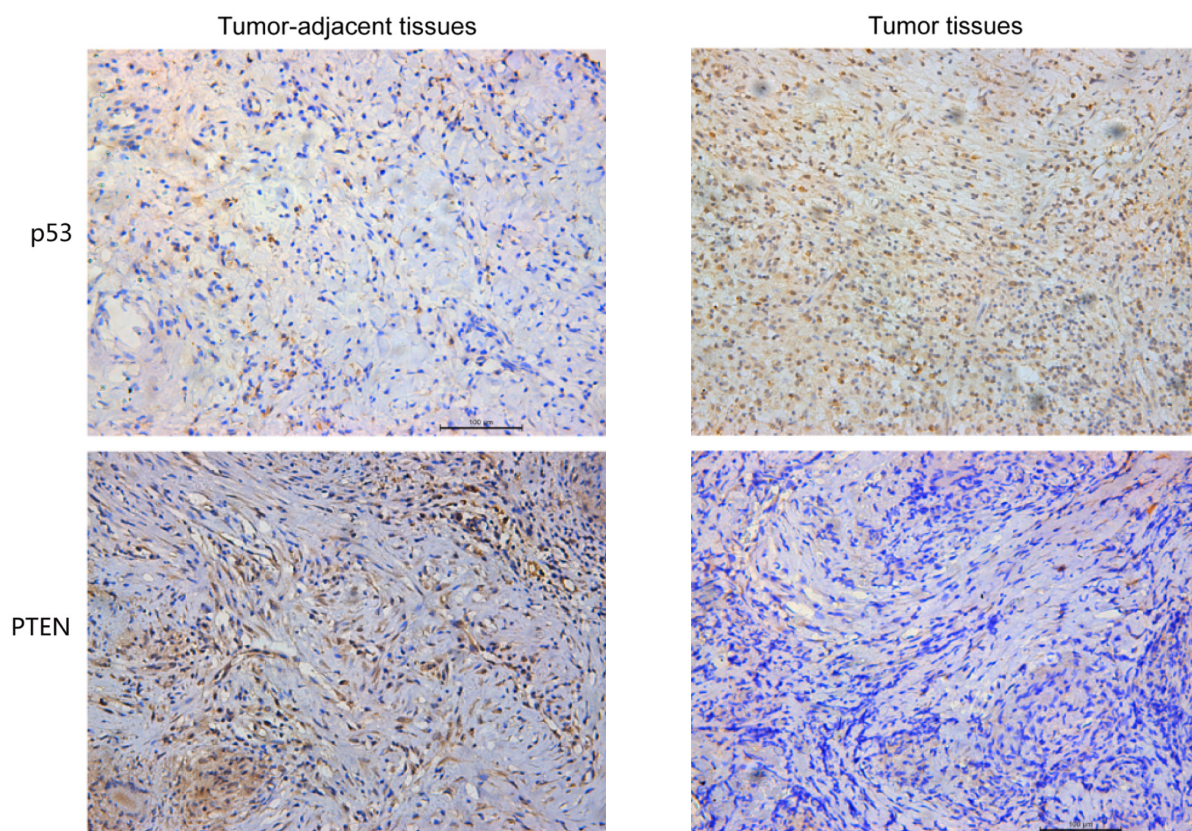


Figure 2. Immunohistochemical expressions of p53 and PTEN in tumor tissues and tumor-adjacent tissues (magnification x40). The expressions of p53 and PTEN protein in tumor tissues were significantly higher than in tumor-adjacent tissues ($p < 0.05$).

Examination of GBM with MRI

As shown in Figure 3, the signal of DWI suggested that it was significantly increased in the tumor, and the ADC was decreased compared to those in the tumor-adjacent area. MRS indicated that the wave section of Cho in the tumor was significantly increased, NAA was significantly decreased, and Cr section was reduced.

Analysis on differences of MRS and ADC in the tumor and the tumor-adjacent area

Table 2 shows that the ratios of Cho/NAA and Cho/Cr of metabolic index in the tumor were higher than those in the tumor-adjacent area, while the ratio of NAA/Cr in the tumor was lower than that in the tumor-adjacent area ($p < 0.05$).

Correlation of p53 with MRS and ADC

The correlation analysis (Table 3) suggested that p53 in the tumor and the tumor-adjacent area was negatively correlated with ADC in the corresponding area ($p < 0.05$). Cho/NAA and Cho/Cr in the tumor were positively correlated with the level of p53 in the tumor, while Cho/NAA and Cho/Cr in the tumor-adjacent area were negatively correlated with the level of p53 in the tumor ($p < 0.05$). NAA/Cr in the tumor was irrelevant to the level of p53 ($p < 0.05$).

Correlation of the level of PTEN with MRS and ADC

Table 4 shows that the level of PTEN in the tumor and the tumor-adjacent area was positively correlated with ADC in corresponding area, while

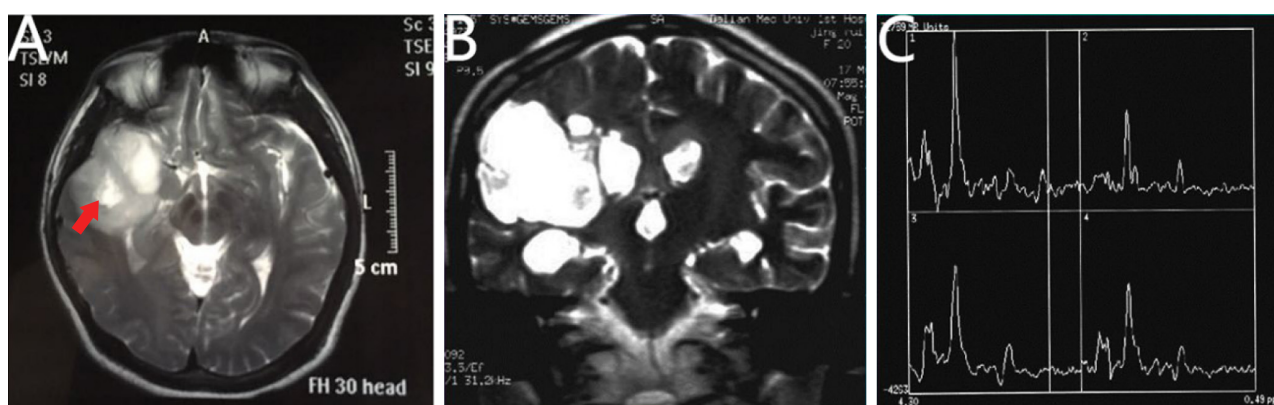


Figure 3. Examination of GBM with MRI. **A and B:** The signal of DWI suggested that it was significantly increased in the tumor and the apparent diffusion coefficient (ADC) was decreased compared with those in the tumor-adjacent area. Arrow shows the tumor. **C:** MRS indicated that the wave section of the Cho in the tumor was significantly increased, NAA was significantly decreased and Cr section was reduced.

Table 1. Comparisons of optical density of p53 and PTEN in the tumor and the tumor-adjacent tissues

Index	Tumor-adjacent tissues (n=38)	Tumor tissues (n=38)	t value	p value
p53	132.5±42.8	472.1±97.5	7.43	0.0012
PTEN	379.4±83.6	86.2±39.2	4.27	0.0027

Table 2. Analysis of differences of MRS and ADC in the tumor and the tumor-adjacent area

Item	Tumor-adjacent area (n=38)	Tumor (n=38)	t value	p value
Cho/NAA	1.62±0.41	3.48±0.73	5.87	0.0018
Cho/Cr	1.53±0.52	3.20±0.66	5.05	0.0043
NAA/Cr	1.76±0.47	0.83±0.25	3.27	0.015
ADC ($\times 10^3 \text{mm}^2/\text{s}$)	2.04±0.43	1.27±0.35	6.34	0.0027

Table 3. Correlation of the level of p53 with MRS and ADC

Index	Level of p53 in the tumor-adjacent area		Level of p53 in the tumor	
	<i>r value</i>	<i>p value</i>	<i>r value</i>	<i>p value</i>
Cho/NAA	0.903	<0.05	0.753	<0.05
Cho/Cr	1.238	<0.05	0.815	<0.05
NAA/Cr	0.104	>0.05	0.443	>0.05
ADC	-0.836	<0.05	-0.644	<0.05

Table 4. Correlation of the level of PTEN with MRS and ADC

Index	Level of PTEN in the tumor-adjacent area		Level of PTEN in the tumor	
	<i>r value</i>	<i>p value</i>	<i>r value</i>	<i>p value</i>
Cho/NAA	-1.633	<0.05	-0.817	<0.05
Cho/Cr	-0.814	<0.05	-1.252	<0.05
NAA/Cr	0.221	>0.05	0.711	>0.05
ADC	1.354	<0.05	0.9425	<0.05

Cho/NAA and Cho/Cr in the tumor were negatively correlated with the level of PTEN in the tumor-adjacent area, and those in the tumor-adjacent area were negatively correlated with the level of PTEN in the tumor ($p < 0.05$). NAA/Cr in the tumor was irrelevant to the level of PTEN ($p < 0.05$).

Discussion

GBM is a highly lethal brain tumor with unique clinical history and molecular characteristics [8]. GBM is mainly manifested as primary and secondary subtypes. Primary GBM subtype is an acute disease with high frequency of gene mutations of epidermal growth factor receptor (EGFR), PTEN and inhibitor of CDK4/alternative reading frame (INK4a/ARF), while secondary GBM subtype evolves from low-level mutation to mutations of platelet derived growth factor (PDGF) and p53 [9].

The p53 gene is divided into wild and mutant type. Wild p53 is a tumor suppressor characterized by short half-life, while mutant p53 can be permanently activated as a carcinogen [10]. When the cell is damaged, wild p53 can induce DNA-damaged cells to enter G1/G0 stationary stage to inhibit cell proliferation, until the damaged DNA is repaired. If this fails, wild p53 will induce apoptosis of damaged cells. The deficiency or mutation of wild p53 will lead to permanent activation of p53, thus failing to effectively activate damage

stress response of downstream DNA, and losing the effect of regulating tumor growth [11,12]. As a tumor-suppressing protein, PTEN has dual specific phosphatase activity, and can mediate the stability of p53 [13]. Studies have shown that PTEN can inhibit murine double minute 2 (MDM2)-mediated p53 degradation through dephosphorylation of phosphatidylinositol 3, 4, 5-trisphosphate (PIP3) and negative regulation of phosphatidylinositol 3, 4, 5-trisphosphate (PIP3)/protein kinase (AKT), which facilitates the induction of mutations or death of irreparable damaged cells [14]. On the contrary, as human PTEN promoter contains the p53 binding site, p53 can induce the transcription of the PTEN gene and increase the level of PTEN protein in the cell [15]. Therefore, p53 and PTEN are also closely related to each other. Both of them play important roles in the inhibition of occurrence and development of tumors.

Sequencing studies on 35 patients with primary GBM conducted by Ohgaki et al. [16] showed that typical p53 mutation was observed in 10 patients (29%), and PTEN missense mutation, insertion, deletion or splice mutations were observed in 14 patients (40%). Moreover, 6 patients of those with typical p53 mutation were accompanied by PTEN mutation or homozygous deletion. The similarity between our experimental results and these studies is that mutant p53 protein in GBM tissues is increased significantly, while PTEN is signifi-

cantly decreased compared with those in GBM-adjacent tissues.

The symptoms of typical malignant GBM are increased intracranial pressure or focal neurologic deficits. It is manifested as high signal of DWI and low signal of ADC in the tumor in terms of DWI. This is because the cell density in the tumor is higher than that in the tumor-adjacent area, and the high signal dispersion of DWI in the tumor is limited [17]. The similarity between data of this experiment and this principle is that ADC in the tumor is higher than that in the tumor-adjacent area. In addition, studies have shown that the average of ADC in GBM is $1.52 \times 10^3 \text{ mm}^2/\text{s}$, while that in malignant GBM is $1.23 \times 10^3 \text{ mm}^2/\text{s}$ [18]. The ADC of the 38 patients with GBM in this study was $1.27 \times 10^3 \text{ mm}^2/\text{s}$, which meets the clinicopathological grading for patients. Analysis on the correlation of PTEN and p53 with ADC also showed that PTEN in the tumor and the tumor-adjacent area was positively correlated to ADC in the corresponding area respectively, while p53 in the tumor and the tumor-adjacent area was negatively correlated with ADC in the corresponding area.

Some studies have shown that the sensitivity, specificity and accuracy of MRS in the diagnosis

of GBM are 100, 86 and 96%, respectively [19]. As paraplasmic glial cells destroy normal neurons, the typical manifestations of MRS in patients with GBM are significant increase in Cho, significant reduction in NAA and moderate or significant decrease in Cr [20]. The results of this study are consistent with the typical characteristics of MRS for GBM. Further analysis showed that Cho/NAA and Cho/Cr were positively correlated with the level of p53 in the tumor, but negatively correlated with PTEN in the tumor. However, the ratio of NAA/Cr in the tumor was not related to the levels of PTEN and p53.

Conclusions

In summary, this study showed that DWI and MRS were significantly correlated with the inactivation or mutation of PTEN and p53 in patients with GBM. The assessment of variability of PTEN and p53 with the values of ADC, Cho/NAA and Cho/Cr has relatively high diagnostic value.

Conflict of interests

The authors declare no conflict of interests.

References

1. Baritchii A, Jurj A, Soritau O et al. Sensitizer drugs for the treatment of temozolomide-resistant glioblastoma. *JBUON* 2016;21:199-207.
2. Van Meir EG, Hadjipanayis CG, Norden AD, Shu HK, Wen PY, Olson JJ. Exciting new advances in neuro-oncology: The avenue to a cure for malignant glioma. *CA Cancer J Clin* 2010;60:166-93.
3. Zheng H, Ying H, Yan H et al. P53 and Pten control neural and glioma stem/progenitor cell renewal and differentiation. *Nature* 2008;455:1129-33.
4. Yilaz SS, Biray AC, Dodurga Y, Ozlem DSZ, Oktar N, Gunduz C. Downregulation of miR-195 via cyclosporin A in human glioblastoma cells. *JBUON* 2015;20:1337-40.
5. Li B, Cai W, Lv D et al. Comparison of MRS and DWI in the diagnosis of prostate cancer based on sextant analysis. *J Magn Reson Imaging* 2013;37:194-200.
6. Heusner TA, Kuemmel S, Koeninger A et al. Diagnostic value of diffusion-weighted magnetic resonance imaging (DWI) compared to FDG PET/CT for whole-body breast cancer staging. *Eur J Nucl Med Mol Imaging* 2010;37:1077-86.
7. Haddadin IS, McIntosh A, Meisamy S et al. Metabolite quantification and high-field MRS in breast cancer. *NMR Biomed* 2009;22:65-76.
8. Carlsson SK, Brothers SP, Wahlestedt T. Emerging treatment strategies for glioblastoma multiforme. *EMBO Mol Med* 2014;6:1359-70.
9. Kim SM, Lim JY, Park SI et al. Gene therapy using TRAIL-secreting human umbilical cord blood-derived mesenchymal stem cells against intracranial glioma. *Cancer Res* 2008;68:9614-23.
10. Chai Y, Xiaoyu L, Haiyan W. Correlation between expression levels of PTEN and p53 genes and the clinical features of HBsAg-positive liver cancer. *JBUON* 2017;22:942-6.
11. Hu W, Zhang C, Wu R, Sun Y, Levine A, Feng Z. Glutaminase 2, a novel p53 target gene regulating energy metabolism and antioxidant function. *Proc Natl Acad Sci U S A* 2010;107:7455-60.
12. Zhang C, Lin M, Wu R et al. Parkin, a p53 target gene, mediates the role of p53 in glucose metabolism and the Warburg effect. *Proc Natl Acad Sci U S A* 2011;108:16259-64.
13. Salmena L, Carracedo A, Pandolfi PP. Tenets of PTEN tumor suppression. *Cell* 2008;133:403-14.
14. Puzio-Kuter AM, Castillo-Martin M, Kinkade CW et al. Inactivation of p53 and Pten promotes invasive bladder cancer. *Genes Dev* 2009;23:675-80.
15. Li X, Xie W, Xie C et al. Curcumin modulates miR-19/PTEN/AKT/p53 axis to suppress bisphenol A-induced

- MCF-7 breast cancer cell proliferation. *Phytother Res* 2014;28:1553-60.
16. Ohgaki H, Dessen P, Jourde B et al. Genetic pathways to glioblastoma: A population-based study. *Cancer Res* 2004;64:6892-9.
 17. Bennett KM, Hyde JS, Rand SD et al. Intravoxel distribution of DWI decay rates reveals C6 glioma invasion in rat brain. *Magn Reson Med* 2004;52:994-1004.
 18. Perez-Torres CJ, Engelbach JA, Cates J et al. Toward distinguishing recurrent tumor from radiation necrosis: DWI and MTC in a Gamma Knife--irradiated mouse glioma model. *Int J Radiat Oncol Biol Phys* 2014;90:446-53.
 19. Schupp DG, Merkle H, Ellermann JM, Ke Y, Garwood M. Localized detection of glioma glycolysis using edited ¹H MRS. *Magn Reson Med* 1993;30:18-27.
 20. Zoula S, Herigault G, Ziegler A, Farion R, Decors M, Remy C. Correlation between the occurrence of ¹H-MRS lipid signal, necrosis and lipid droplets during C6 rat glioma development. *NMR Biomed* 2003;16:199-212.